

In search of smooth sandpiles: the Edwards-Wilkinson equation with flow

Parthapratiim Biswas*, Arnab Majumdar†, Anita Mehta‡
S.N.Bose National Centre For Basic Sciences
Salt Lake City, Block JD, Sector III, Calcutta-700 091, INDIA

J.K.Bhattacharjee§
Indian Association for the Cultivation of Science
Jadavpur, Calcutta-700 032, INDIA

Abstract

The well-known Edwards-Wilkinson equation with a flow term added exhibits a smoothing fixed point in addition to the normal EW fixed point. Based on this, we present a model of sandpiles involving a coupling between fixed and mobile grains, which then shows the smoothing behaviour that would be expected to obtain after avalanche propagation.

PACS NOS.: 05.40.+j, 05.70.Ln, 46.10.+z, 64.60.Ht

Typeset using REVTeX

*ppb@boson.bose.res.in

†arnab@boson.bose.res.in

‡anita@boson.bose.res.in

§tpjkb@iacs.ernet.in

The dynamics of sandpiles have intrigued researchers in physics over recent years [1,2] with a great deal of effort being devoted to the development of techniques involving for instance cellular automata [3,4], continuum equations [2,5,6] and Monte Carlo schemes [7] to investigate this very complex subject. However what have often been lost sight of in all this complexity are some of the extremely simple phenomena that are exhibited by granular media that still remain unexplained.

One such phenomenon is that of the smoothing of a sandpile surface after the propagation of an avalanche [8]. It is clear what happens physically: an avalanche provides a means of shaving off roughness from the surface of a sandpile by transferring grains from bumps to available voids [4], and thus leaves in its wake a smoother surface. However, surprisingly, researchers have not to our knowledge come up with a model of sandpiles that has exhibited this behaviour.

In this paper we present therefore a very simple model involving coupled continuum equations which exhibits smoothing. In work that is presently under completion [9], we have constructed a cellular automaton model of a sandpile surface where this smoothing behaviour is also made manifest.

This paper comprises : (i) an introductory section, where the equations are presented and explained (ii) a section where numerical and analytical results are obtained (iii) a concluding section where the physics of our results is discussed.

I. INTRODUCTION: THE EQUATIONS

Coupled equations have been seen to be immensely helpful in representing the dynamics of systems where there are *two* clear relaxational mechanisms, for instance those corresponding respectively to particles moving independently of each other and to their collective motion within clusters [2,6]. In the case of sandpiles, these mechanisms correspond respectively to the intercluster and intracluster motion of individual grains [5].

The model we present here involves just such a pair of coupled equations, where the equation governing the evolution of clusters (“stuck” grains) is closely related to the very well-known Edwards-Wilkinson (EW) model [10]. The equations are:

$$\begin{aligned}\frac{\partial h}{\partial t} &= D_h \nabla^2 h + c \nabla h + \eta(x, t) \\ \frac{\partial \rho}{\partial t} &= D_\rho \nabla^2 \rho - c \nabla h\end{aligned}\tag{1}$$

where the first of the equations describes the height $h(x, t)$ of the sandpile surface at (x, t) measured from some mean $\langle h \rangle$, and is precisely the EW equation in the presence of the flow term $c \nabla h$. The second equation describes the evolution of flowing grains, where $\rho(x, t)$ is the local density of such grains at any point (x, t) . As usual, the noise $\eta(x, t)$ is taken to be Gaussian so that:

$$\langle \eta(x, t) \eta(x', t') \rangle = \Delta^2 \delta(x - x') \delta(t - t').$$

with Δ the strength of the noise. Here, $\langle \dots \rangle$ refers to an average over space as well as over noise.

Before further analysis, we review some general facts about rough interfaces [11]. Three critical exponents, α , β , and z , characterise the spatial and temporal scaling behaviour of

a rough interface. They are conveniently defined by considering the (connected) two-point correlation function of the heights

$$S(\mathbf{x} - \mathbf{x}', t - t') = \langle h(\mathbf{x}, t) h(\mathbf{x}', t') \rangle - \langle h(\mathbf{x}, t) \rangle \langle h(\mathbf{x}', t') \rangle. \quad (2)$$

We have

$$S(\mathbf{x}, 0) \sim |\mathbf{x}|^{2\alpha} \quad (|\mathbf{x}| \rightarrow \infty) \quad \text{and} \quad S(\mathbf{0}, t) \sim |t|^{2\beta} \quad (|t| \rightarrow \infty), \quad (3)$$

and more generally

$$S(\mathbf{x}, t) \approx |\mathbf{x}|^{2\alpha} F(|t|/|\mathbf{x}|^z) \quad (4)$$

in the whole long-distance scaling regime (\mathbf{x} and \mathbf{t} large). The scaling function F is universal in the usual sense; α and $z = \alpha/\beta$ are respectively referred to as the roughness exponent and the dynamical exponent of the problem.

In addition, we have for the full structure factor which is the double Fourier transform $S(k, \omega)$

$$S(k, \omega) \sim \omega^{-1} k^{-1-2\alpha} \Phi(\omega/k^z) \quad (5)$$

which gives in the limit of small k and ω ,

$$S(k, \omega = 0) \sim k^{-1-2\alpha-z} \quad (k \rightarrow 0) \quad \text{and} \quad S(k = 0, \omega) \sim \omega^{-1-2\beta-1/z} \quad (\omega \rightarrow 0) \quad (6)$$

The scaling relations for the corresponding single Fourier transforms are

$$S(k, t = 0) \sim k^{-1-2\alpha} \quad (k \rightarrow 0) \quad \text{and} \quad S(x = 0, \omega) \sim \omega^{-1-2\beta} \quad (\omega \rightarrow 0) \quad (7)$$

II. NUMERICAL AND ANALYTICAL RESULTS

A. Analysis of the decoupled equation: the Edwards-Wilkinson equation with flow

For the purposes of analysis, we focus on the first of the two coupled equations (Eq.1) presented above,

$$\frac{\partial h}{\partial t} = D_h \nabla^2 h + c \nabla h + \eta(x, t) \quad (8)$$

noting that this equation is essentially decoupled from the second. (This statement is, however, not true in reverse, which has implications to be discussed later). We note that this is entirely equivalent to the Edwards-Wilkinson equation [10] in a frame moving with velocity c

$$x' = x + ct, \quad t' = t$$

and would on these grounds expect to find only the well-known EW exponents $\alpha = 0.5$ and $\beta = 0.25$ [10]. This would be verified by naive single Fourier transform analysis of Eq.8 which yields these exponents via Eq.7.

Eq.8 can be solved exactly as follows. Using the standard form

$$\hat{L}h = \eta(x, t)$$

with

$$\hat{L} = [\frac{\partial}{\partial t} - D_h \nabla^2 - c \nabla]$$

we find for the propagator $G(k, \omega)$

$$G = (-i\omega + D_h k^2 + ikc)^{-1}$$

This can be used to evaluate the structure factor

$$S(k, \omega) = \frac{\langle h(k, \omega) h(k', \omega') \rangle}{\delta(k + k') \delta(\omega + \omega')} \quad (9)$$

which is the Fourier transform of the full correlation function:

$$G(x - x', t - t') = \langle h(x, t) h(x', t') \rangle. \quad (10)$$

The solution for $S(k, \omega)$ so obtained is:

$$S(k, \omega) = \frac{\Delta^2}{(\omega - ck)^2 + D_h^2 k^4} \quad (11)$$

This is illustrated in Fig.1 while representative graphs for $S(k, \omega = 0)$ and $S(k = 0, \omega)$ are presented in Figs.2 and 3 respectively. It is obvious from the above that $S(k, \omega)$ does not show simple scaling. More explicitly, if we write

$$S^{-1}(k, \omega = 0) = \frac{\omega_0^2}{\Delta^2} \left(\frac{k}{k_0} \right)^2 \left[1 + \left(\frac{k}{k_0} \right)^2 \right]$$

with $k_0 = c/D_h$, and $\omega_0 = c^2/D_h$, we see that there are two limiting cases :

- for $k \gg k_0$, $S^{-1}(k, \omega = 0) \sim k^4$; using again $S^{-1}(k = 0, \omega) \sim \omega^2$, we obtain $\alpha = 1/2$ and $\beta = 1/4$, $z = 2$ via Eqs.6.
- for $k \ll k_0$, $S^{-1}(k, \omega = 0) \sim k^2$; using the fact that the limit $S^{-1}(k = 0, \omega)$ is always ω^2 , this is consistent with the set of exponents $\alpha = 0$, $\beta = 0$ and $z = 1$ via Eqs.6.

The first of these contains no surprises, being the normal EW fixed point, [10] while the second represents a new, ‘smoothing’ fixed point.

We now explain this smoothing fixed point with a simple physical picture. The competition between the two terms in Eq.8 determines the nature of the fixed point observed: when the diffusive term dominates the flow term, the canonical EW fixed point is obtained, in the limit of large wavevectors k . On the contrary, when the flow term predominates, the effect of diffusion is suppressed by that of a travelling wave whose net result is to penalise large slopes; this leads to the smoothing fixed point obtained in the case of small wavevectors k .

We add in passing that this crossover would not have been as transparently obvious had we been using the single Fourier transforms $S(k, t = 0)$ and $S(x = 0, \omega)$ for numerical purposes. We illustrate this by writing explicitly the expressions for the relevant quantities:

$$S(k, t = 0) \sim \frac{1}{k^2} \quad (12)$$

$$S(x = 0, \omega) \sim \frac{1}{\omega^2} \quad \text{for } \omega \text{ small} \quad (13)$$

$$S(x = 0, \omega) \sim \frac{1}{\omega^{1.5}} \quad \text{for } \omega \text{ large} \quad (14)$$

The examination of $S(k, t = 0)$ (Fig.4) on its own yields no indication of the crossover to the smoothing fixed point, while only a detailed examination of the $S(x = 0, \omega)$ graph (Fig.5a) reveals this, indicating a crossover from $\omega^{-1.5}$ at high frequencies to ω^{-2} at low frequencies. Clearly, though this is more time-consuming to obtain, the double Fourier transform, ie the full structure factor, provides a much more unambiguous picture of the crossover in this problem.

Additionally, the investigation of even the single Fourier transform to detect the crossover is not without its complexities. The detection of the smoothing fixed point, characterised by $z = 1$, needs a careful investigation of the low frequency part of $S(x = 0, \omega)$. This is elaborated on in Appendix A, where we discuss the anomalous oscillatory behaviour obtained to do with the competition between grid sizes and some characteristic lengths in this problem (Appendix B).

In view of the above, it is preferable to use the double Fourier transform to obtain an unambiguous picture of the structure factor although this strategy might on first appearance seem to be a computational overkill. The overwhelming advantage is that, by scanning the structure factor as a function of frequency ω for a fixed k , one immediately sets two frequency scales ck and $D_h k^2$, thus making it possible to pick up the relevance of these scales in $S(k, \omega)$.

Before turning to an interesting physical application of the two fixed points in our linear equation, we mention in passing that our discussion is equally applicable to the Kardar-Parisi-Zhang (KPZ) equation [12] with the addition of a flow term. Here too, the use of the double Fourier transform reveals the presence of the ‘smoothing’ fixed point due to the flow term [13].

B. Coupled equations: a model of smoothing

Returning to the coupled equations (1), we realise from the above that the interface h is smoothed because of the action of the flow term which penalises the sustenance of finite gradients ∇h . As we have seen from the above analysis, this is indeed the case for the equation in h , which is effectively decoupled from the equation in ρ . However, the equation in ρ is manifestly coupled to h so we would need to ensure that no instabilities are generated in this, in order for the coupled equations to qualify as a valid model of sandpile dynamics.

In this spirit, we look first at the value of ρ averaged over the pile, as a function of time (Fig.6a). We observe that the incursions of $\langle \rho \rangle$ into negative values are limited to relatively small values, suggesting that the addition of a constant background of ρ exceeding this negative value would render the coupled system meaningful, at least to a first approximation.

In order to ensure that this average over the pile does not involve wild fluctuations over the body of the pile, we examine the fluctuations in ρ , viz. $\sqrt{\langle \rho^2 \rangle - \langle \rho \rangle^2}$ (Fig.6b). The trends in that figure indicate that this quantity appears to saturate, at least upto computationally accessible times. Finally we look at the *minimum* value of ρ at any point in the pile over a large range of times (Fig.6c); this appears to be bounded by a modest (negative) value of ‘bare’ ρ . Our conclusions are thus that the fluctuations in ρ saturate at computationally accessible times and that the negativity of the fluctuations in ρ can always be handled by starting with a constant ρ_0 , a constant ‘background’ of flowing grains, which is more positive than the largest negative fluctuation.

Physically, then, the above implies that at least in the presence of a constant large density ρ_0 of flowing grains, it is possible to induce the level of smoothing corresponding to the fixed point $\alpha = \beta = 0$. This model is thus one of the simplest possible ways in which one can obtain a representation of the smoothing that is frequently observed in experiments on real sandpiles after avalanche propagation [8].

III. CONCLUSIONS

In conclusion we have presented a very simple model of sandpile dynamics which manifests the interfacial smoothing commonly observed after avalanche propagation, both in experiments [8] and physically in sand dunes. This consists simply of a set of coupled continuum equations [2,5] which model the exchange process between the stuck grains at the interface h and the flowing grains ρ which flow across the interface. The equation in h is closely related to the well-known Edwards-Wilkinson equation [10], modifying this simply by the addition of a flow term which penalises excess gradients across the interface, and thereby causes the smoothing.

We find, on analysing the equations, that there are two fixed points which characterise the interface equation: one, the normal diffusive fixed point corresponding to $\alpha = 1/2$, $\beta = 1/4$ and $z = 2$, and the other, the new smoothing fixed point corresponding to $\alpha = 0$, $\beta = 0$ and $z = 1$. We mention here that the first of these is the one that would also be observed in the frame of the avalanche moving with the flow velocity c , while the smoothing would only be observed in the stationary frame of an observer, who would observe the smoother surface left in the wake of the avalanche.

Finally, in work that is in progress, we have observed quantitatively this smoothing phenomenon in a cellular automaton model of sandpiles [9]. We hope that this will motivate actual experiments to measure more quantitatively this so far qualitatively observed and intuited behaviour at sandpile surfaces.

ACKNOWLEDGEMENTS

Arnab Majumdar acknowledges the hospitality of SNBNCBS during the course of this work, while Anita Mehta acknowledges valuable discussions with Prof. Sir Sam Edwards during its initiation.

APPENDIX A: OSCILLATIONS

We explain here the origins of the observed oscillations in the structure factor $S(x=0, \omega)$. The single Fourier transform $S(x, \omega)$ is defined by

$$S(x=0, \omega) = \frac{1}{2\pi} \int_{-\infty}^{\infty} S(k, \omega) \exp(ikx) dk \quad (\text{A1})$$

In the limit of small ω the integral can be written as:

$$S(x=0, \omega) = \frac{1}{2\pi} \int_{-\infty}^{\infty} \frac{1}{Dk^2} \delta(\omega - ck) dk \quad (\text{A2})$$

This is the origin of the ballistic behaviour of the flow term and is responsible in part for some of the observed oscillations, as we explain below. It is clear from Eqs.13 and 14 that the crossover from small to large ω for $x=0$ should not involve any imaginary quantities, and therefore strictly speaking we should not see any oscillatory behaviour in the structure factor in this limit. However it is important to realise that the full form of the structure factor $S(x, \omega)$ for finite x *does* contain imaginary portions, in order to understand fully the origin of the obtained oscillations.

The characteristic length and time scales in our problem are given by (Appendix B)

$$t_0 = \frac{D}{c^2} \text{ and } x_0 = \frac{D}{c}$$

Whenever grid sizes in time or space are comparable to these characteristic lengths, the profile fluctuates across these intervals, which is then aggravated by the shock fronts associated with the flow term. This results in:

- oscillatory behaviour arising from the *non-zero* intervals in x associated with the sampling of the profile to generate the Fourier transform, $S(x=0, \omega)$, which introduce a flavour of $S(x, \omega)$ for *finite* x .
- oscillations which become increasingly violent as c increases because of the increased fluctuations associated with the ballistic flow term over the grids.

This line of reasoning is borne out by the following table:

Parameters	Grid Sizes & Characteristic Lengths	Observation
$c=1 \ D_h = 1$	$\Delta x = 0.5, x_0 = 1.0$ $\Delta t = 0.001, t_0 = 1.0$	No Oscillation . Fig.5a
$c=5 \ D_h = 1$	$\Delta x = 0.1, x_0 = 0.2$ $\Delta t = 0.001, t_0 = 0.04$	Oscillation(1 peak). Fig.5b
$c=10 \ D_h = 1$	$\Delta x = 0.1, x_0 = 0.1$ $\Delta t = 0.001, t_0 = 0.01$	Oscillation(2 peaks). Fig.5c

Thus in order to avoid these oscillations, one should choose grid sizes Δx and Δt in such a way that they are always less than the characteristic scales in the problem, i.e.,

$$\Delta x \ll x_0 \quad \text{and} \quad \Delta t \ll t_0.$$

APPENDIX B: LENGTH AND TIME SCALES OF INTEREST

The Edwards-Wilkinson equation with a flow term ($c\nabla h$) is given by

$$\frac{\partial h}{\partial t} = D_h \nabla^2 h + c \nabla h + \eta(x, t) \quad (\text{B1})$$

with

$$\langle \eta(x, t) \eta(x', t') \rangle = \Delta^2 \delta(x - x') \delta(t - t')$$

We perform a scale change in order to make this equation dimensionless using

$$t = t_0 T, \quad x = x_0 X, \quad h = h_0 H$$

and obtain

$$\frac{\partial H}{\partial T} = D'_h \frac{\partial^2 H}{\partial X^2} + c' \frac{\partial H}{\partial X} + \delta_0 \xi \quad (\text{B2})$$

where,

$$D'_h = D_h \frac{t_0}{x_0^2}, \quad c' = c \frac{t_0}{x_0}, \quad \delta_0 = \frac{\Delta}{h_0} \sqrt{\frac{t_0}{x_0}}$$

and

$$\langle \xi(X, T) \xi(X', T') \rangle = \delta(X - X') \delta(T - T')$$

Next we make a choice of the scales (x_0 , t_0 and h_0) such that the coefficients D'_h , c' and δ_0 are unity. This gives the following scales

$$t_0 = \frac{D_h}{c^2}, \quad x_0 = \frac{D_h}{c}, \quad h_0 = \frac{\Delta}{\sqrt{c}} \quad (\text{B3})$$

An estimate of the exponent z can be made by considering the diffusion and flow term separately. Substituting L for x_0 along with the condition $D'_h = c' = 1$ we realise that on length scales comparable to the system size, L , the associated time scale for diffusion is L^2/D_h and that for flow is given by L/c . The physical meaning of these time scales is the time taken for the diffusive and flow-like correlations to span the system. This is the time ($t_\times \sim L^z$) for crossover to the saturated regime. Clearly the above time scales indicate $z = 2$ for diffusion-dominated behaviour and $z = 1$ for flow-dominated behaviour respectively.

REFERENCES

- [1] Anita Mehta and G.C.Barker, Rep. Prog. Phys. **57**, 383 (1994); H.M.Jaeger and S.R.Nagel, Science **255**, 1523 (1992); H. M. Jaeger, S. R. Nagel and R. P. Behringer, Rev. Mod. Phys. **68**, 1259 (1996).
- [2] *Granular Matter: An Interdisciplinary Approach*, ed. Anita Mehta (Springer Verlag, New York, 1993).
- [3] P.Bak, C.Tang, and K.Wiesenfeld, Phys. Rev. Lett. **59**, 381 (1987); Phys. Rev. **A 38**, 364 (1988).
- [4] Anita Mehta and G.C.Barker, Europhys. Lett. **27**, 501 (1994).
- [5] Anita Mehta, J.M.Luck, and R.J.Needs, Phys.Rev. **E 53**, 92 (1996).
- [6] Anita Mehta, R.J. Needs, and S. Dattagupta, J. Stat. Phys. **68**, 1131 (1992); J.P. Bouchaud, M.E. Cates, J. Ravi Prakash, and S.F.Edwards, J. Phys. I France **4**, 1383 (1994); Phys. Rev. Lett. **74**, 1982 (1995).
- [7] Anita Mehta and G.C.Barker, Phys. Rev. Lett. **67**, 394 (1991).
- [8] S.R.Nagel, private communication.
- [9] G.C.Barker and Anita Mehta, to be published (1997).
- [10] S.F.Edwards and D.R.Wilkinson, Proc. Roy. Soc. London **A 381**, 17 (1982).
- [11] T.Halpin-Healy and Y.C.Zhang, Phys. Rep. **254**, 215 (1995); J.Krug and H.Spohn ,in *Solids far from Equilibrium*, ed.C. Godréche (Cambridge University Press,1992).
- [12] M.Kardar, G.Parisi, and Y.Zhang, Phys. Rev. Lett. **56**, 889 (1986).
- [13] Parthapratim Biswas, Arnab Majumdar, Anita Mehta and J.K.Bhattacharjee, to be published (1997).

FIGURES

FIG. 1. The double Fourier transform, $S(k = k_i, \omega)$ for the h - h correlation function for three wavevectors $k_1 = 0.02$, $k_2 = 0.08$ and $k_3 = 0.12$. ($c = 2$ and $D_h = \Delta^2 = 1.0$)

FIG. 2. The double Fourier transform, $S(k, \omega = 0)$ for the h - h correlation function, along with a fit to $(k^{2.00 \pm 0.03} + k^{4.00 \pm 0.05})^{-1}$. ($c = D_h = \Delta^2 = 1.0$)

FIG. 3. The double Fourier transform, $S(k = 0, \omega)$ for the h - h correlation function, along with a fit to $\omega^{-2.00 \pm 0.05}$. ($c = D_h = \Delta^2 = 1.0$)

FIG. 4. The single Fourier transform $S(k, t = 0)$ for the h - h correlation function, along with a power-law fit to $k^{-1.97 \pm 0.02}$.

FIG. 5. (a) The single Fourier transform $S(x = 0, \omega)$ for the h - h correlation function, along with a power-law fit to $\omega^{-1.97 \pm 0.05}$ for small ω and $\omega^{-1.48 \pm 0.02}$ for large ω . (b) and (c) show the oscillatory behaviour (see Appendix A) of $S(x = 0, \omega)$ near the crossover region. The oscillations increase with increasing c , as can be seen from a comparison of Fig. (b) ($c = 10$) and Fig. (c) ($c = 5$). $D_h = \Delta^2 = 1.0$ throughout.

FIG. 6. Curves relating to the behaviour of the equation in ρ (Eq.1) over 10^6 timesteps. (a) shows the behaviour of the mean $\langle \rho \rangle$ as a function of time, where the average over the sandpile was computed over a sample configuration. (b) shows the variance ρ_{rms} of ρ as a function of time. This was computed for 100 configurations over the sandpile surface. (c) shows the bounds of the fluctuations in ρ , ρ_{min} and ρ_{max} , as a function of time.

Fig.1

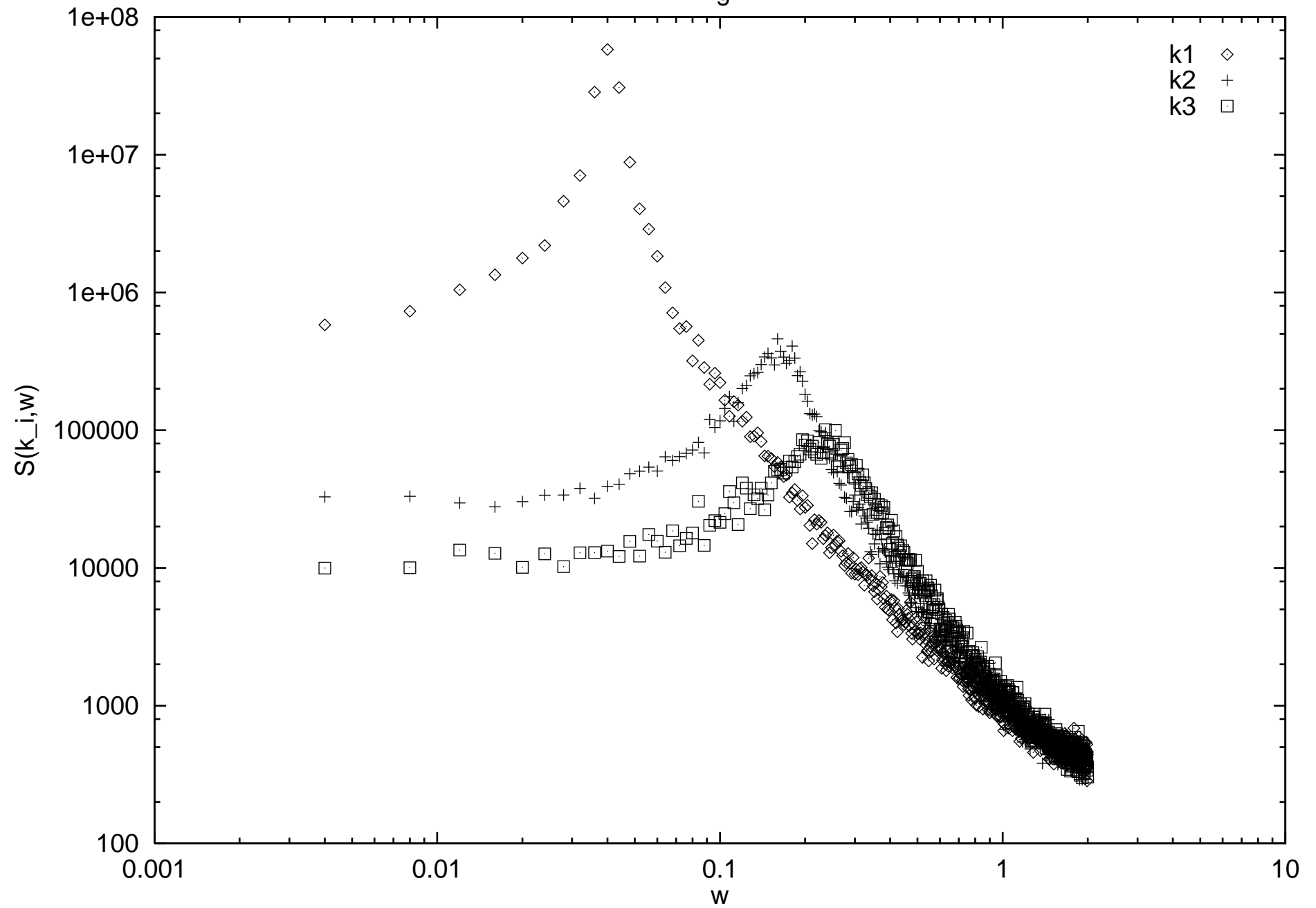


Fig.2

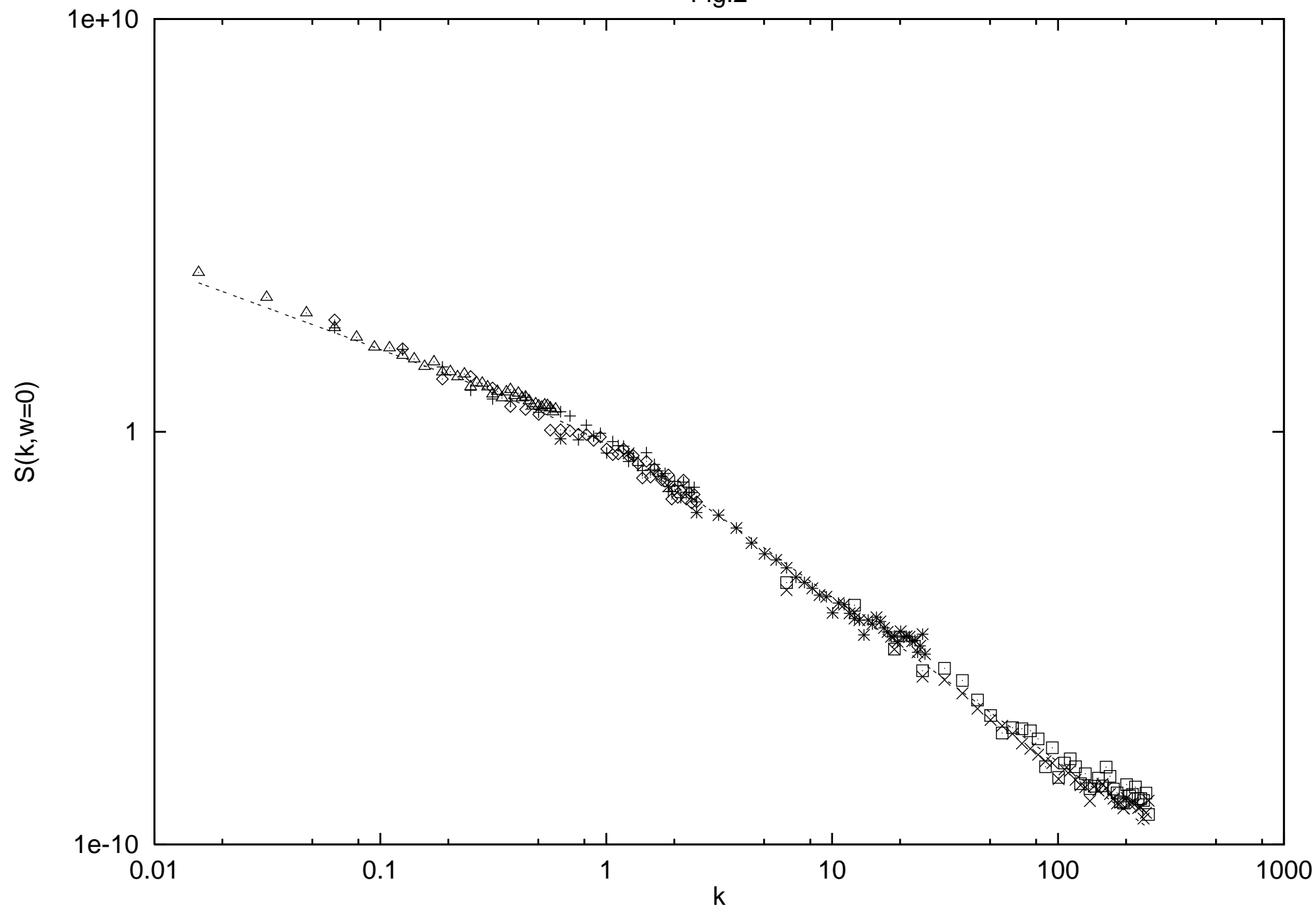


Fig.3

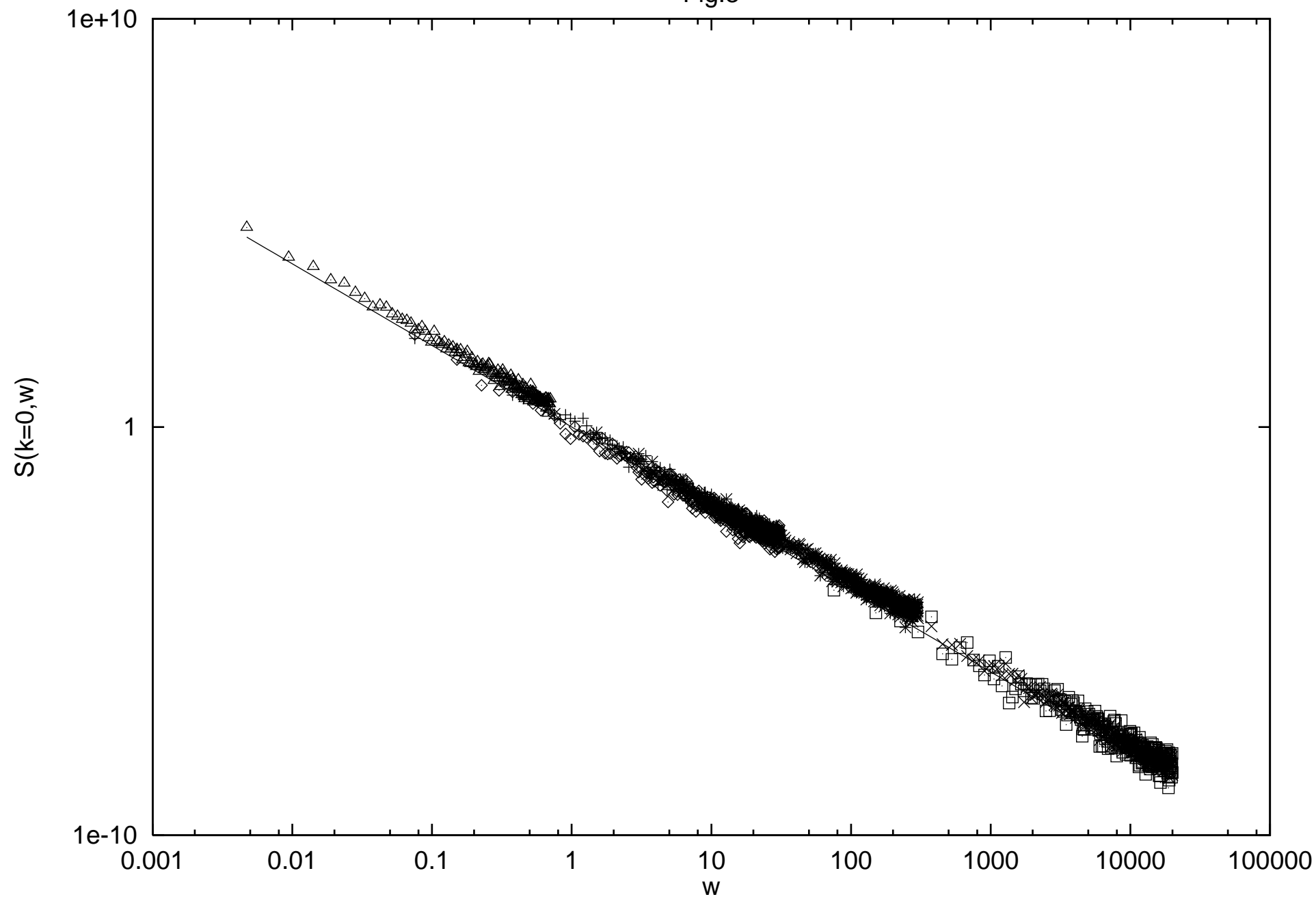


Fig.4

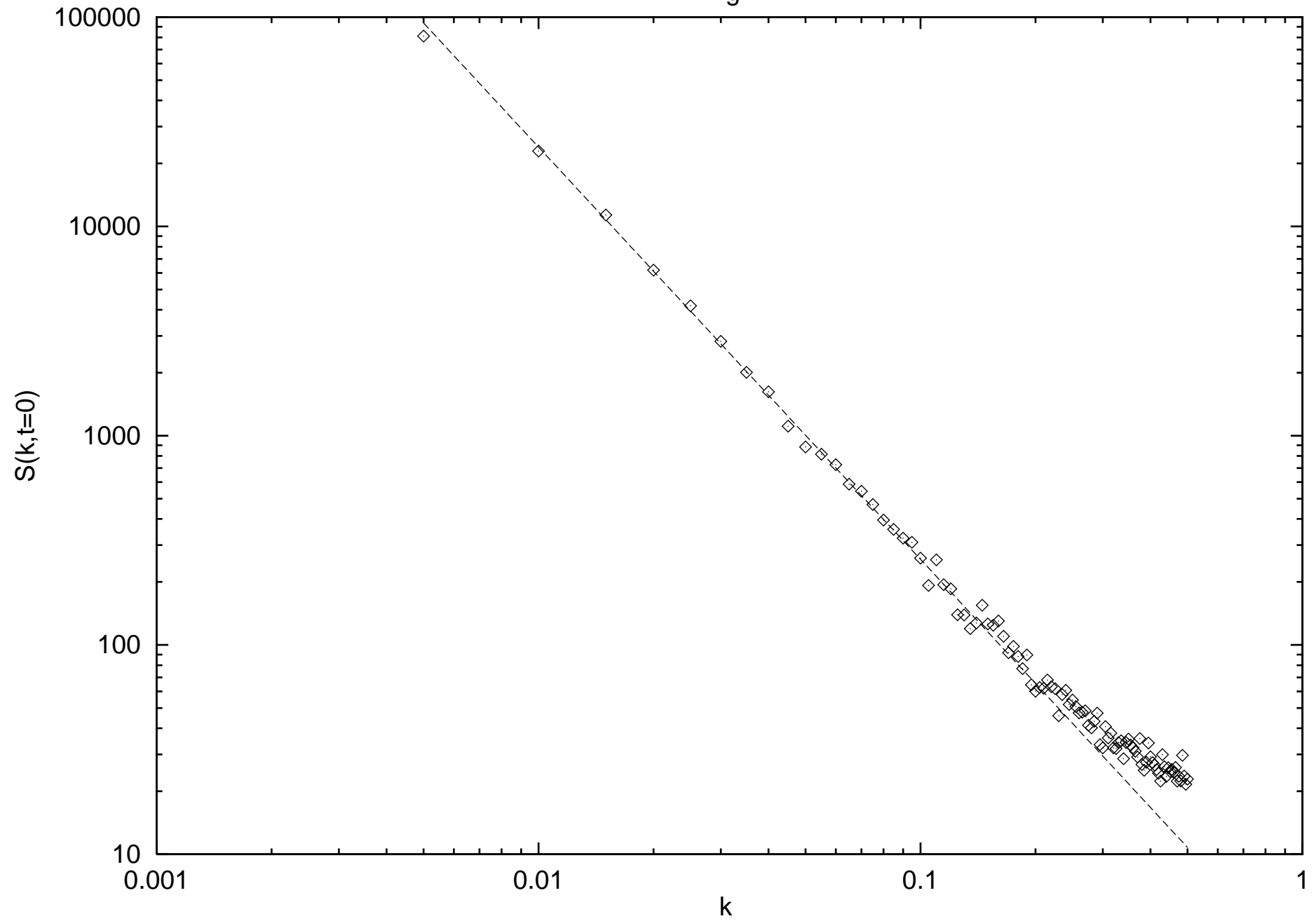


Fig.5a

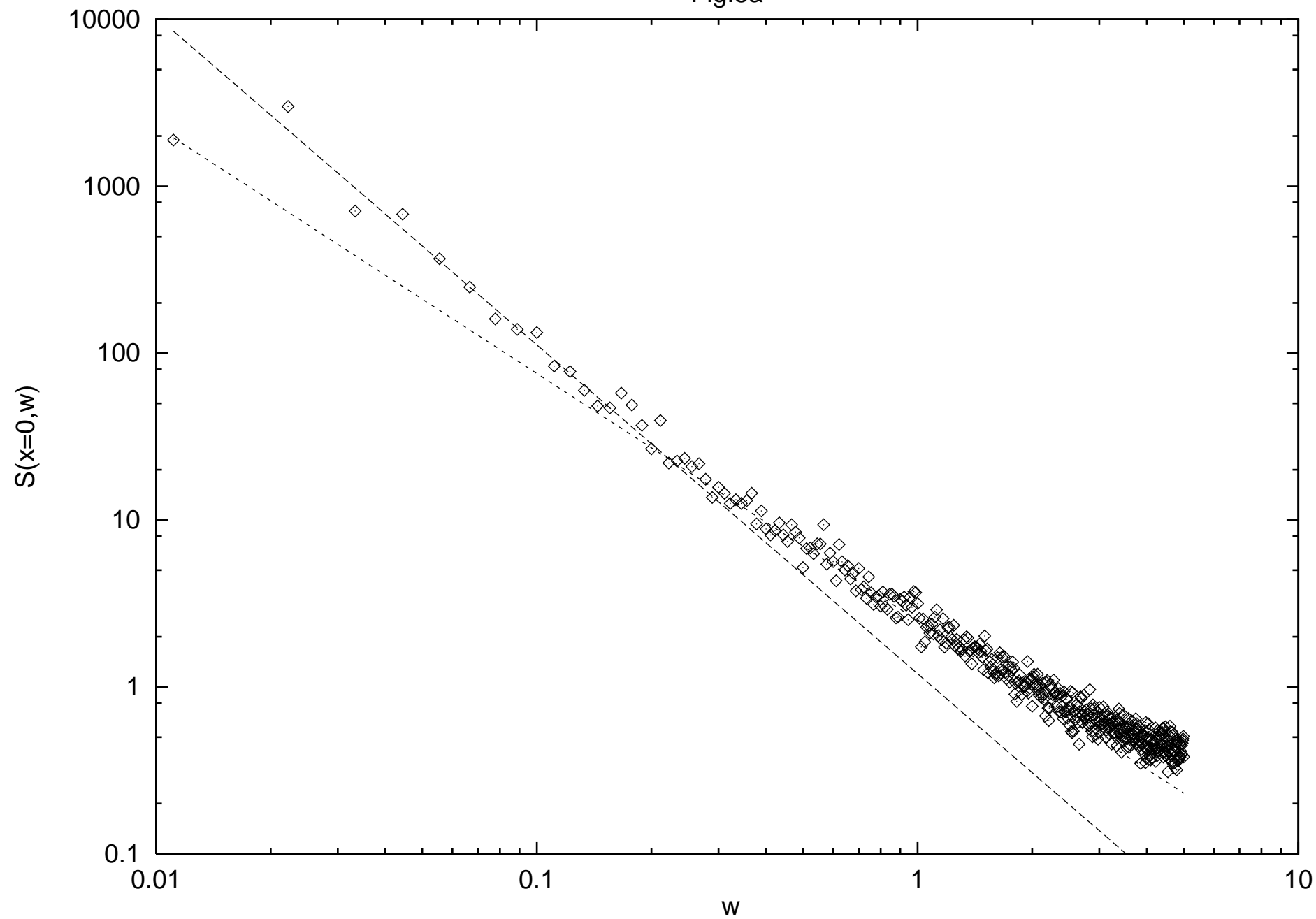


Fig.5b

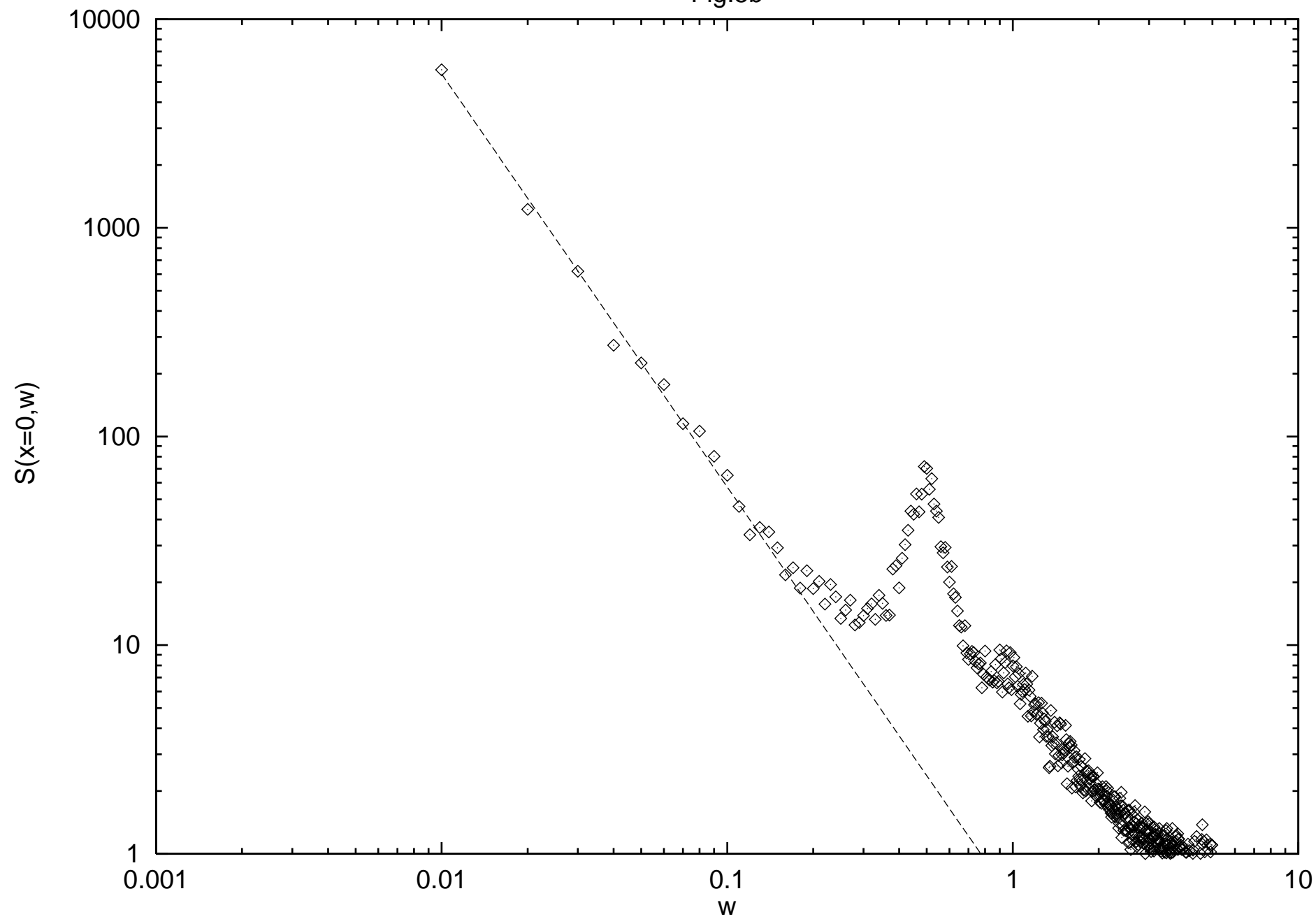


Fig.5c

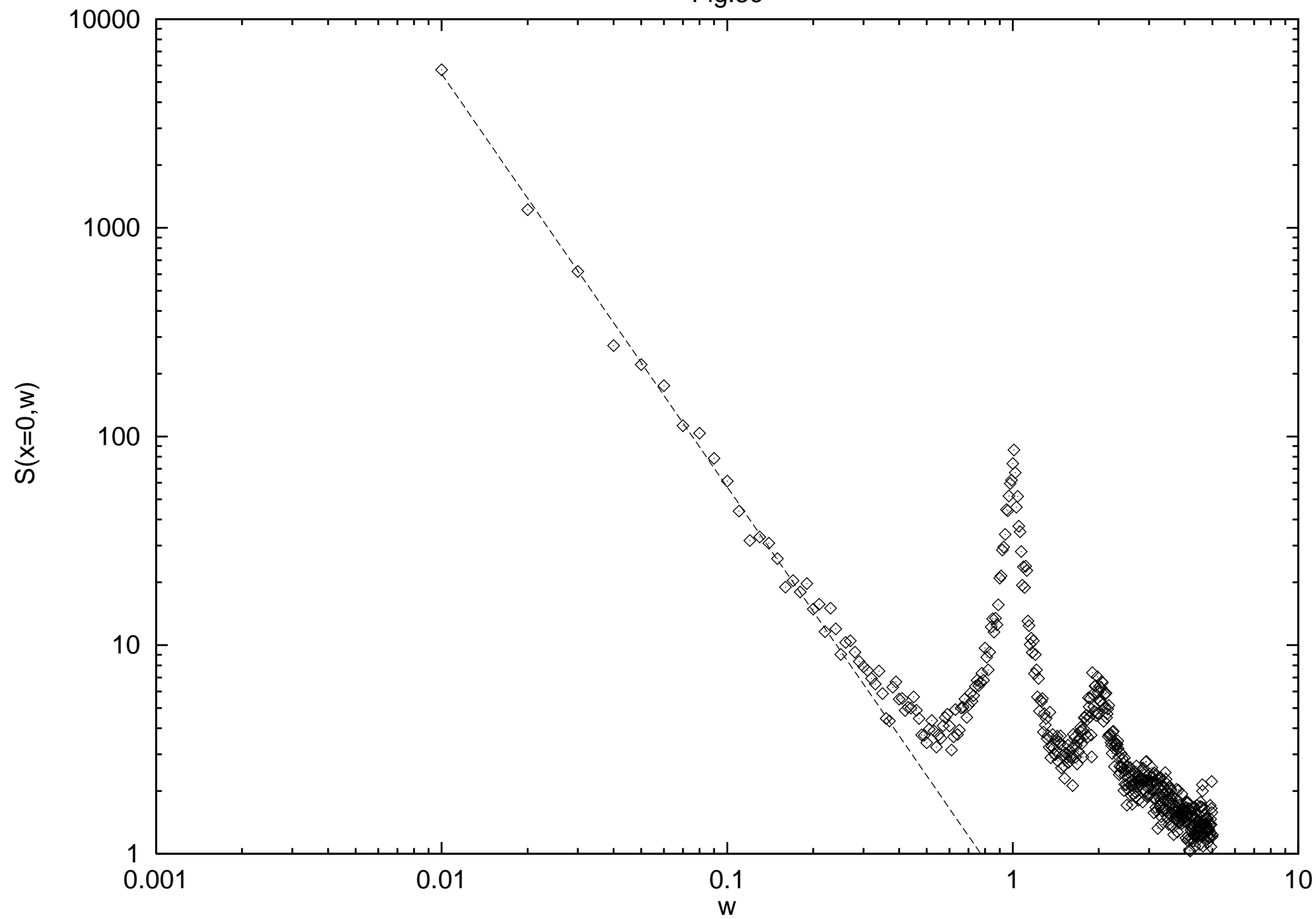


Fig.6a

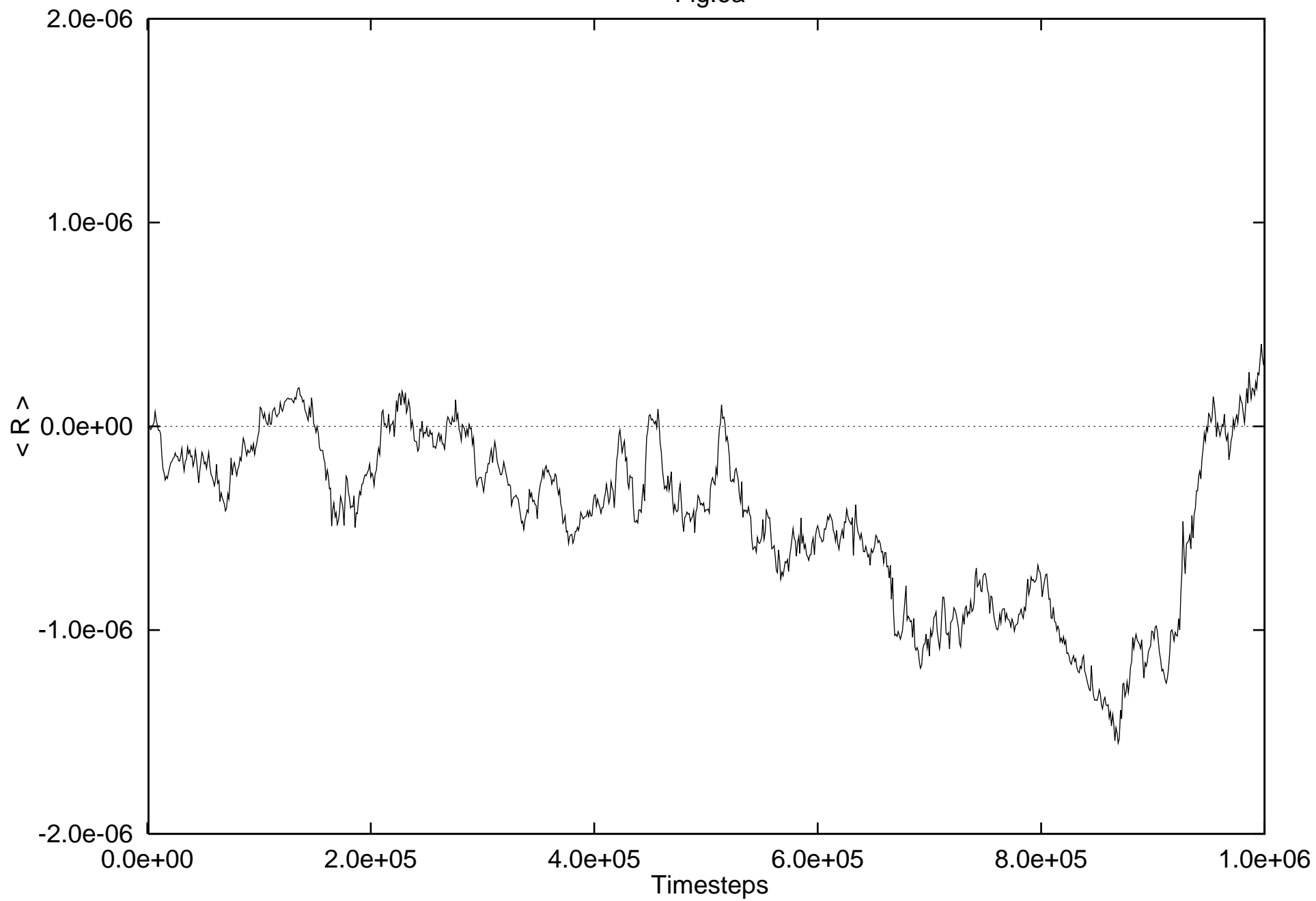


Fig.6b

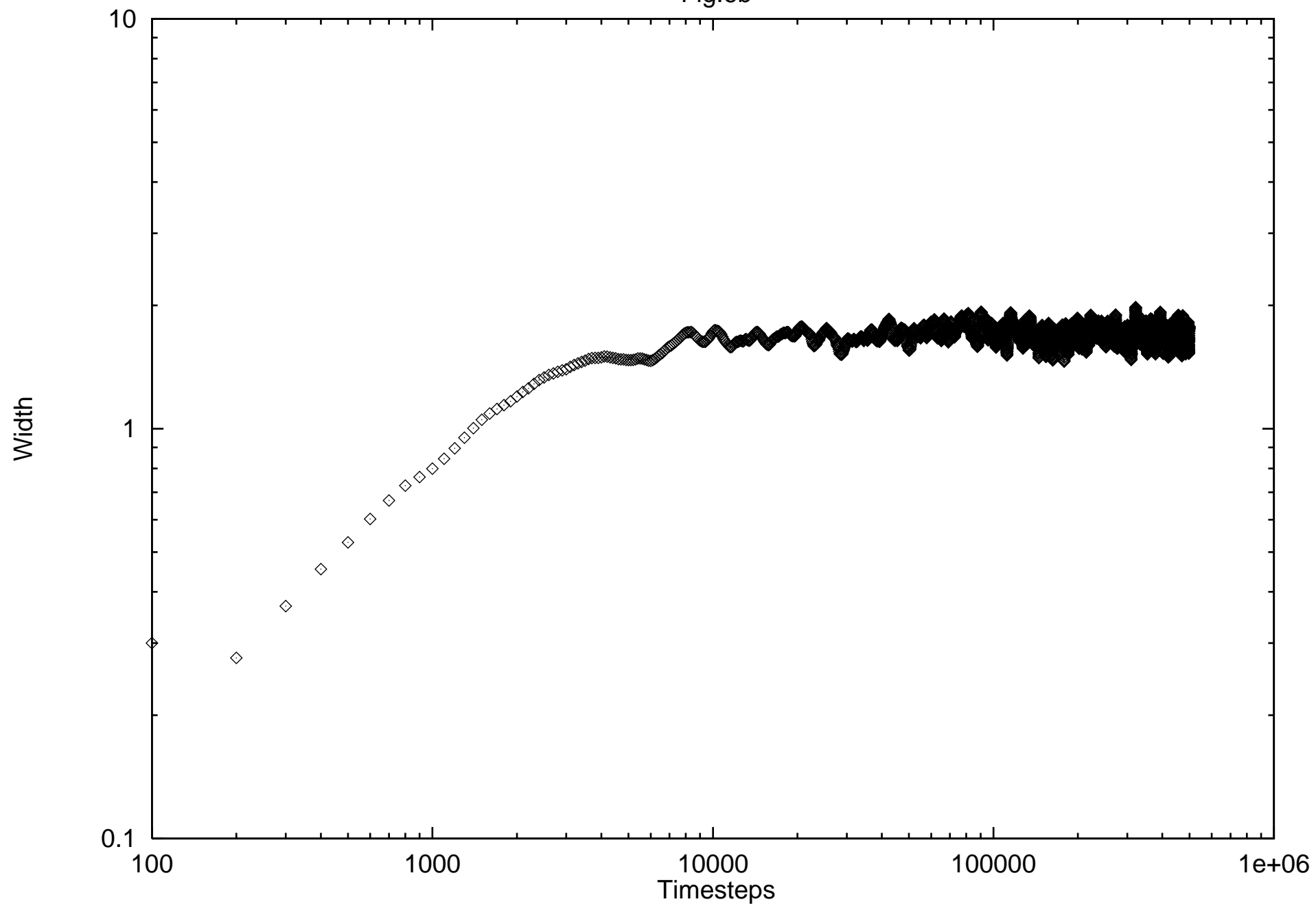


Fig.6c

